Artificial neural network and genetic algorithms for modeling of removal of an azo dye on walnut husk

Abuzer Çelekli[a,*], Hüseyin Bozkurt[b], Faruk Geyik[c]

[a]Faculty of Art and Science, Department of Biology, University of Gaziantep, Gaziantep, Turkey 27310, Tel. +903423171925; Fax: +903423601032; email: celekli.a@gmail.com
[b]Faculty of Engineering, Department of Food Engineering, University of Gaziantep, Gaziantep 27310, Turkey, email: hbozkurt@gantep.edu.tr
[c]Faculty of Engineering, Department of Industrial Engineering, University of Gaziantep, Gaziantep 27310, Turkey, email: fgeyik@gantep.edu.tr

ABSTRACT

The study dealt with an evaluating kinetic aspect of removal of Basic Red (BR) 46 by walnut husk (*WH*). Artificial neural network (ANN), gene expression programming (GEP), logistic, and pseudo-second-order kinetic models were constructed to predict the removal efficiency of BR 46 on *WH*. Spectra of *WH* before and after the sorption process were obtained using FTIR–ATR. Functional groups such as hydroxyl, carbonyl, and carboxyl groups had a significant role on the interaction between *WH* and BR 46. Maximum sorption was determined as 66.45 mg g^{-1}. About 2,160 experimental mean sets were used to feed ANN structure. ANN was found to be the best model due to its lowest error and highest determination of coefficient values. ANN showed that contact time was the most efficient parameter, followed by initial dye concentration for the sorption process. GEP model successfully described the sorption kinetic process as functions of pH, adsorbent particle size, initial dye concentration, contact time, and temperature in a single equation. Results of thermodynamic parameters indicated that this process is being feasible, endothermic, and spontaneous. Results revealed that *WH* had a great potential to remove BR 46 from aqueous solution at different environmental conditions.

Keywords: Artificial neural network; Basic Red 46; Gene expression programming; Sorption; Walnut husk

1. Introduction

In this twenty-first century, millions of people throughout the world are suffering from shortage of fresh and clean drinking water which is polluted by waste disposal. Contamination of aquatic ecosystems with recalcitrant compounds has become a major global problem [1–3]. Xenobiotic in ecosystems threaten earth because of their adverse effects on all forms of life [1–3]. Therefore, great attentions have been given for the removal of recalcitrant compounds from wastewater, during the last few years.

Azo dyes have synthetic origin and complex aromatic structure, which make them more stable and resistant to heat, oxidizing agents, photodegradation,

*Corresponding author.

and biodegradation [2,3]. They account for approximately 70% of all dyestuffs, which are extensively used in the textile, paper, food, leather, cosmetics, and pharmaceutical industries [1–3]. About 10–15% of industrial dyes in effluents are discharged into receiving water bodies [1–3]. They pose a threat to environmental safety and affect aquatic organisms by impeding light penetration, causing aesthetic problems, and toxicity to life [2,3]. Moreover, contaminated stream with this effluent is sometimes used for irrigation of agricultural fields. By this way, recalcitrant compounds not only may affect the growth of these plants, but also accumulate in them, which may lead to their transfer into organisms and human beings [2].

Diverse physical, chemical, physicochemical, and biological techniques have been used for the treatment of wastewater [1–5]. These processes are complicated and have high labor cost, moreover, some of these methods require additional chemicals and/or produce further toxic products [1–3]. Also, removal of recalcitrant azo dyes completely from effluents is very hard using treatment procedures because of their color fastness, stability, and resistance to degradation [2,3]. Therefore, there is a demand for the effective, low-cost, and eco-friendly technologies to remove these dyes from aqueous effluents. Among treatment technologies, sorption process has received a lot of attention due to its simplicity and high efficiency, as well as the availability of a wide range of adsorbents.

Many biological materials, especially agricultural residues have been investigated for the removal of dyestuffs [6–12]. For this purpose, walnut shell has been used for the removal of chromium [13,14], removal of cesium [15], sorption of methylene blue [16], and sorption of Lanaset Red G [17]. In the literature, walnut husk (*WH*) has not been previously used for the sorption of azo dyes.

Wastewater treatment systems consist of multi-input variables and output(s) (dye adsorbed per unit of adsorbent at *t* time and at equilibrium). Prediction of water quality as output(s) from a water treatment plant is very difficult as input water quality changes continuously. Modeling of sorption process by the use of ANN techniques is quite appropriate to solve these complex issues [18–23]. ANN is a technique inspired by biological neuron processing design as computer-based systems [18]. In the last decade, this technique has been successfully used for describing adsorption systems [19–21] and biodegradation of dyes [22,24]. ANN gives information about relative importance of parameters driving on sorption kinetics or biodegradation of dyes [20,22,24].

Genetic algorithm has been used for finding precise or approximate solutions to optimize or search problems. Similar to genetic algorithm, the genetic programming needs a problem to define. Genetic programming, empirical models, have been developed by Ferreira [25] as gene expression programming (GEP). Parameters derived from mathematical models can be converted into information for the removal of pollutant [26]. These parameters provide knowledge about the adsorption behavior and they are used in the design of wastewater treatment systems.

Basic dyes are widely used for dyeing of acrylic, nylon, silk, and wool. Basic Red 46 (BR 46) is a synthetic azo dye containing –N=N– bonds and widely used in the textile industry. BR 46 has the positive charge delocalized throughout the chromophoric system and has an affinity toward the negatively charged functional groups on materials.

Turkey ranked fourth in the world's walnut production in 2005. *WH*, available in large quantities, is usually used as firewood, resulting air pollution. Thus, the use of this waste for different purposes can play a significant role for solving the disposal problems. In addition, utilization of waste materials can contribute to wise and efficient use of materials, to protect environment, and to improve the balance of trade by reducing the dependence on imported materials. Azo dyes are the most problematic dye, as they tend to pass through conventional treatment systems. *WH* waste as an effective and low-cost adsorbent has not been previously used for removing an azo dye, BR 46. The objective of this study was (i) to investigate sorption efficiency at different particle size, adsorbent dosage, initial pH value, temperature, initial dye concentration, and contact time for removing BR 46 on *WH*, (ii) to develop three-layer ANN model, (iii) to investigate sorption behavior using logistic and pseudo-second-order kinetic models, and (iv) to develop an unique model to describe whole of the studied factors by GEP model.

2. Materials and methods

2.1. Adsorbent

WH was obtained from a field crop in the southeastern region of Turkey. Collected sample was washed twice with tap water. Dried adsorbent was grounded in a mortar, sieved using different mesh sizes into three particles sizes (125–250, 250–500, and >500 μm mesh sizes), and stored in air-tight polyethylene bottle up to study time. Chemical pretreatment was not applied prior to sorption experiments.

Infrared spectra of the adsorbent before and after BR 46 sorption were taken using a Fourier transform infrared (FTIR) spectrometer equipped with an

attenuated total reflection (ATR) accessory (Perkin–Elmer Spectrum 100 FTIR–ATR Spectrometer).

2.2. Adsorbate

Dye used in this study is C.I. BR 46 (CAS 12221-69-1; $C_{18}H_{21}N_6Br$, MW = 403.32 g mol^{-1}) obtained from a textile factory in Gaziantep, Turkey. The chemical structure and properties of this dye is given in Table 1. Stock dye solution (1 g L^{-1}) was prepared by dissolving accurately weighed quantity of BR 46 in distilled water. Desired dye solutions were prepared by diluting the stock dye solution with a suitable volume of distilled water.

2.3. Sorption studies

Full factorial design was used to investigate whole effects of three different particle sizes (>500–125 μm), four different initial pHs (pH 7–10), five different initial dye concentrations (20–100 mg L^{-1}), twelve contact time (0–210 min), and three different temperatures (293–313 K) on sorption of BR 46 onto *WH*. Sorption experiments were performed as duplicate. The mean sample size was 2,160.

The pH of solution was adjusted to the desired value by adding 0.1-M HCl and/or 1.0-M NaOH solutions. Experiments were carried out with 100 mL sorption solution (with desired dye concentration and pH) and desired adsorbent concentration in 250-mL conical flask. These flasks were agitated by placing it in the orbital shaker at 150 rpm for 210 min.

During sorption studies, withdrawn samples were centrifuged to precipitate suspended biomass at 5,000 rpm for 5 min. Residual BR 46 concentration in

the supernatant was analyzed using spectrophotometer (Jenway 6305) at 530 nm. Each data point was the mean of two independent samples.

In this study, q_t shows the amount of BR 46 adsorbed on *WH* at time t (mg g^{-1}) calculated using Eq. (1).

$$q_t = \frac{(C_o - C_t) \times V}{m} \qquad (1)$$

where C_o and C_t represent the dye concentrations (mg L^{-1}) at initial and at time t, respectively. V is the volume of solution (L) and m is the mass of adsorbent (g L^{-1}).

2.4. Kinetic modeling

Pseudo-second-order kinetic, logistic, ANN, and genetic programming models were used to investigate the sorption of BR 46 on *WH*. The sorption of BR 46 on *WH* was also studied under the aspects of thermodynamic studies.

Pseudo-second-order kinetic model [27] is one of the mostly used kinetic models to describe kinetic sorption data. This kinetic model was used and represented as:

$$\frac{t}{q_t} = \frac{1}{kq_e^2} + \frac{t}{q_e} \qquad (2)$$

where q_e and q_t show the dye adsorbed on the adsorbent (mg g^{-1}) at equilibrium and at time t (min). k is the pseudo-second-order rate constant.

Logistic, a sigmoidal, model has been proposed to obtain more information and describe all sorption

Table 1
General characteristics of Basic Red 46

Name of dye	Basic Red 46
Chemical formula	$C_{18}H_{23}N_6Br$
Molar mass	403.32 g mol^{-1}
Color Index name	Basic Red 46
CAS Number	12221-69-1
λ_{max}	530 nm
Chemical structure	
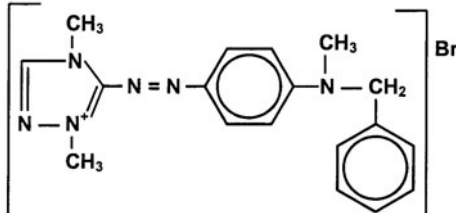
process [28]. This model was fitted to the experimental data within the sorption period and expressed as:

$$q_t = \frac{A}{\left\{1 + \left(\frac{t}{B}\right)^Z\right\}} \tag{3}$$

where A is maximum sorption value (asymptote value) at equilibrium; t is time (min). B and Z are logistic constants. The nonlinear fitting procedure was performed using commercial computer software SigmaPlot version 11 (Systat Sofware, Inc., CA, USA) via the Marquardt–Levenberg algorithm.

ANNs are high-performance, nonlinear analytical tools that have used a network topology weighing relationship between inputs and output(s). A multilayered network was trained to perform a particular (activation) function by adjusting the values of the connections (weights) between elements (neurons). The connections (input) coming to a neuron were summed by the summation function ($NetX_i$) and added the bias (b_i, a constant weight of a neuron representing the generalization error), expressed in (Eq. (4)). The activation function ($f(x)$) produces an output (O_j) using $NetX_i$. Logistic transfer function given in Eq. (5) was used as an activation function.

$$NetX_i = \sum_{j=1}^{n} w_{ij}x_j + b_i \tag{4}$$

$$O_i = f(x) = \frac{1}{1 + e^{-(NetX_i)}} \tag{5}$$

where x_j is value of input j at input layer and w_{ij} is the corresponding weight of connection between each neuron (j) in input layer and each neuron (i) in hidden layer, and also between hidden and output layers. The activation function held the final weights between neurons of all network and produced a predicted output as in Eq. (5).

Neural Network Toolbox V4.0 of the MATLAB 7 mathematical software was used for the prediction of sorption efficiency. In this tool, logistic transfer function with back-propagation algorithm at hidden layer and logistic transfer function at output layer activation function were used.

Genetic algorithm is a search technique that has been used for finding precise or approximate solutions for optimization or search problems. Fundamental aim of developing GEP model was to generate the mathematical functions for the prediction of an azo dye sorption on WH. GenXproTools 4.0 Advanced Edition software by Gepsoft was used for the GEP model. The

maximum number of generations for training of the models for the GEP model was between 5,000 and 10,000. The parameters used in the GEP model are presented in Table 2.

2.5. Validation of the models

Applicability of models to describe the sorption process was validated by the coefficient of determination (R^2) and the sum of squares error (SSE) between experimental and predicted data from the models. SSE was used as an error function (Eq. (6)):

$$SSE = \sqrt{\frac{\sum \left(q_{exp} - q_{predict}\right)^2}{N}} \tag{6}$$

where N is the number of data point, q_{exp} and $q_{predict}$ are the observed experimental and predicted data from models, respectively.

3. Results and discussion

3.1. Characterization of adsorbent

Adsorption capacity depends upon the chemical structure of the surface consisting of various functional groups such as amine, hydroxyl, carboxyl, carbonyl, sulfonate, and phosphate, which can bind with dye molecules. In order to discover changes in the surface of adsorbent, FTIR–ATR spectra of WH before and after the sorption of BR 46 are shown in Fig. 1(a) and (b), respectively.

Table 2
Parameters of GEP model

Parameters	Value
Function set	+, −, *, /, Sqrt, Ln, Sin, Cos
Numerical constants	[−10, +10]
Chromosomes	50
Head size	8
Number of genes	5
Linking function	Addition
Fitness function	RRSE
Mutation rate	0,044
Inversion rate	0.1
One-point recombination rate	0.3
Two-point recombination rate	0.3
Gene recombination rate	0.1
Gene transposition rate	0.1
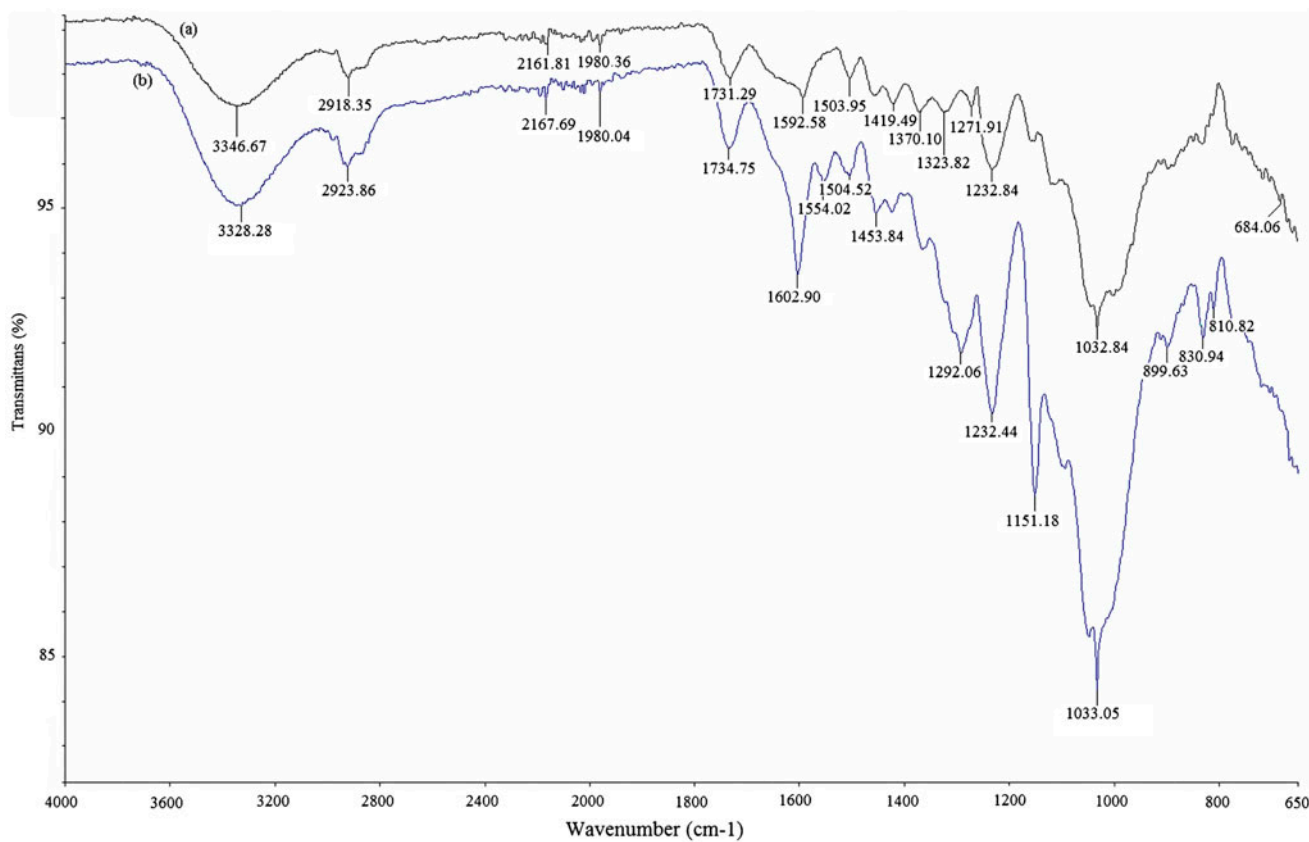
Fig. 1. FTIR spectra of (a) the nature adsorbent and (b) BR 46-loaded adsorbent.

The plot of Fig. 1(a) indicates that several major intense bands, around 3,347, 2,918, 1,731, 1,593, 1,233, and 1,033 cm^{-1} were observed in unloaded adsorbent. The peak at 3,347 cm^{-1} could be assigned to –OH and –NH$_2$ groups [17,29], while the peak at 2,922 cm^{-1} could be attributed to –OH stretching vibrations [8]. The bands at 1,731, 1,593, 1,233, and 1,033 cm^{-1} could be corresponding to carbonyl (C=O) groups; C=N and –NH$_2$ groups; the –C–O stretching; and groups of –C–C [16,29]. FTIR analysis revealed that *WH* has various functional groups such as amine, hydroxyl, carbonyl, and carboxyl groups.

After the sorption of BR 46 on *WH*, shifting of some peaks were observed as 3,328, 2,924, 1,735, 1,603, 1,292, 1,151, and 831 cm^{-1} (Fig. 1(b)). These changes could be due to new bonds formed between *WH* and BR 46 molecules. Functional groups as hydroxyl, carbonyl, and carboxyl groups had a significant role on the interaction between *WH* and BR 46. Similar results were also found for the sorption of BR 46 on canola hull [30] and the removal of two cationic dyes by milled sugarcane bagasse [9].

3.2. Effects of particle size, adsorbent dose, and pH

Adsorbent particle size, dose, and solution pH play important roles on the sorption capacity. Three particle sizes (125–250, 250–500, and >500 μm) of *WH* were conducted to 50-mg L^{-1} BR 46 solution. Amount of adsorbed dye increased with the decrease in particle size due to the increase in surface area and better accessibility of the pores for dye molecules. Grinding of large particles into smaller ones can also open some tiny sealed channels, which can also increase the sorption. The removal of BR 46 was carried out at four different adsorbent doses (0.5, 1.0, 2.0, and 3.0 g L^{-1}). The highest sorption was observed at 1.0-g L^{-1} adsorbent dosage, followed by 0.5 g L^{-1}. The lowest sorption at 3.0 g L^{-1} could be explained as a consequence of partial overlapping or aggregation of adsorbent, which caused decrease in effective surface area to interact with dye molecules. This is in agreement with results of Deniz and Saygıdeğer [31], in which using princess tree leaf and activated carbon from wild olive cores [29] for the sorption of BR 46.

Effect of initial pH values from 1 to 10 on the sorption process were studied at 50-mg L^{-1} BR 46. A tremendous increase ($p < 0.01$) in the sorption capacity was observed at high pH values. Determination of zero point charge (pH$_{zpc}$) of the adsorbent is important to assess the sorption mechanism. Çelekli et al. [17] reported that pH$_{zpc}$ of *WH* was found as 6.1, where electrostatic repulsion between *WH* and BR 46 was minimum. At pH > pH$_{zpc}$, the surface of the adsorbent gets negatively charged, which favored the sorption of BR 46 on *WH* due to electrostatic attraction. Consequently, the highest sorption value was found at pH 10.

3.3. Effects of contact time, initial dye concentration, and temperature

The removal of BR 46 by *WH* was performed at various contact time ($t = 0$–210 min) and initial dye concentration (ranging 20 to 100 mg L^{-1}) at 293, 303, and 313 K (Fig. 2). The sorption of BR 46 (q_t, mg g^{-1}) significantly increased with increasing contact time ($p < 0.01$). Rapid sorption was observed during the first 60 min of contact time due to the abundance of functional groups on *WH* surface. After that, removing rate slowed down gradually until the equilibrium value, where no significant difference ($p > 0.05$) was observed in the amount of adsorbed dye, because of functional groups saturation and entrance of dye molecules into pores.

Increasing initial dye concentration significantly increased ($p < 0.01$) the removal of BR 46. This could be a consequence of increasing the driving force for mass transfer, in agreement with results of previous studies [8,9,22,32]. Additionally, increasing the initial dye concentration could increase the probability of contact between dye molecules and adsorbent.

The sorption was found to be heat dependent, thereby indicating the process was endothermic in nature. This could be due to increasing temperature might have increased the adsorptive forces between dye molecules and surface activity of adsorbent being involved in the sorption process.
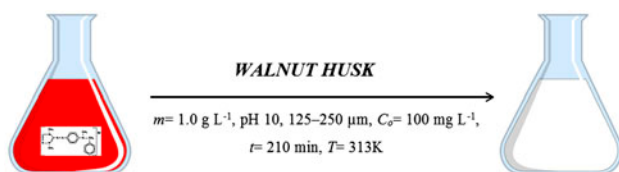
Fig. 2. Sorption of BR 46 on *WH* under various environmental conditions.

3.4. Modeling

Pseudo-second-order kinetic, logistic, ANN, and GEP models were used to investigate sorption of BR 46 on *WH*.

3.4.1. ANN Modeling

A three-layer ANN with a tangent sigmoid transfer function at hidden layer and a linear transfer function at output layer was used in this work (Fig. 3). The input layer had five neurons as particle size, initial pH regime, initial dye concentration, contact time, and temperature. The output layer had one neuron as an amount of adsorbed BR 46 on the adsorbent. Series of topologies were used to determine optimum number of hidden nodes, in which the number of nodes varied from 2 to 40. Increasing number of neurons more than 25 did not make significant difference among SSE values. Therefore, 5 input neurons, 25 hidden neurons, and 1 output, so totally 31 neurons for network structure were selected for training and sets testing. Each topology was repeated three times to avoid random correlation due to random initialization of the weights. About 2,160 experimental mean sets were used to feed ANN structure. Samples were divided into training, validation, and test sets that each of them contains 1,468, 346, and 346 samples, respectively. All inputs were scaled in [−1, +1] interval and the output was scaled in [0, 1] interval.

3.4.2. Simulation of GEP model

Maximum numbers of generations for training of the models for GEP were between 5,000 and 10,000.
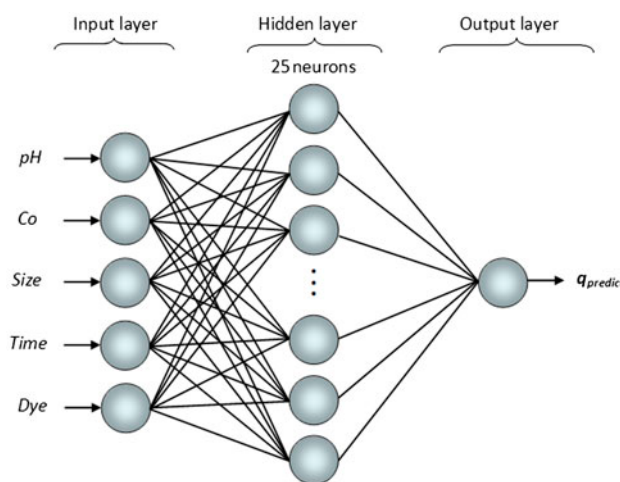
Fig. 3. Optimized ANN architecture for the prediction of sorption of azo basic dye.

According to parameters of GEP, the GEP model was run and the best predictive functions were obtained as Eqs. (7)–(12). The tree expression model is shown in Fig. 4. Results of this model indicated that the values were $c1 = 2.9357$ for $Sub\,ET1$, $c0 = 5.6018$ for $Sub\,ET2$, $c1 = -6.2633$, and $c2 = 2.833$ for $Sub\,ET3$, $c2 = 4.0447$ for $Sub\,ET5$.

The mathematical formulation of the GEP model is expressed as:

$$q_{\text{predict}} = Sub\,ET1 + Sub\,ET2 + Sub\,ET3 + Sub\,ET4 \\ + Sub\,ET5 \tag{7}$$

$$Sub\,ET1 = \text{pH}/\left[(2.9357x\,C_o + \text{size})\big/\sqrt{tx\,C_o}\right] \tag{8}$$

$$Sub\,ET2 = (0.1785x\,T) + \sqrt{C_o} - \cos(\text{pH}) \tag{9}$$

$$Sub\,ET3 = \cos(2.833x(-6.2633)x\,T) + \sqrt{C_o} - \cos(\text{pH}) \tag{10}$$

$$Sub\,ET4 = -6.5864 \tag{11}$$

$$Sub\,ET5 = \sin\left(\sqrt{T}\right)x\cos[\ln(0.2472x\,t)] \tag{12}$$

where q_{predict} is the dye adsorbed on the adsorbent from the model, C_o represents the initial dye concentration, pH is the initial pH value, $size$ is the adsorbent particle size, t is the sorption time, and T is the temperature.

3.4.3. Comparison of sorption kinetic modeling

Results of predictive modeling obtained from pseudo-second-order kinetic, logistic, ANN, and GEP models are given in Table 3. Fittings of kinetic models to the experimental data are given in Fig. 5(a)–(d). A plot of Fig. 5(a) indicated that pseudo-second-order kinetic model had no well fitting to experiment data of higher BR 46 concentrations. On the other hand, logistic (Fig. 5(b)) and ANN (Fig. 5(c)) were more competitive models with higher R^2 and lower SSE values than that of other models (Table 3). Maximum sorption of BR 46 on WH was determined as 66.45 mg g^{-1} from logistic model (Table 3). Maximum adsorption capacities of various adsorbents for BR 46 reported in literature together with that of WH obtained in the present study are represented in Table 4. WH presented satisfactory sorption capacity for the removal of reactive dye compared to canola hull [30], princess tree leaf [31], and Moroccan clay [33]. The sorption capacity of WH was lower than those of activated carbon from wild olive cores treated by H$_3$PO$_4$ [29] and boron waste [34] for the sorption of same azo dye. This could be due to differences in type and amount of functional groups on structures and sorption mechanisms of various adsorbents and experimental conditions. So, WH as a low-cost biological material had a remarkable potential to remove BR 46 from aqueous solution at various operating conditions.

Regression analyses were performed in order to compare experimental (q_{exp}) and predicted (q_{predict}) data from the kinetic models. Results indicated that values of R^2 were found to be 0.9880, 0.9973, 0.9988, and 0.9572 for pseudo-second-order kinetic, logistic, ANN, and GEP models, respectively. Well agreement of ANN was also reported in the literature, in which $R^2 = 0.987$ for the biotreatment of Malachite Green by *Cladophora* species [23], $R^2 = 0.998$ for the prediction of Lanaset Red G on WH [17], $R^2 = 0.953$ for the degradation of Acid Blue 92 on *Lemna minor* [35], $R^2 = 0.978$ for the removal of Reactive Red 141 by an organoclay [36], 0.999 for the prediction of an azo-metal complex dye onto lentil straw [37], $R^2 = 0.998$ for the removal of methylene blue using activated carbon [38], $R^2 = 0.963$ for the removal of methylene blue on the lignite [39],
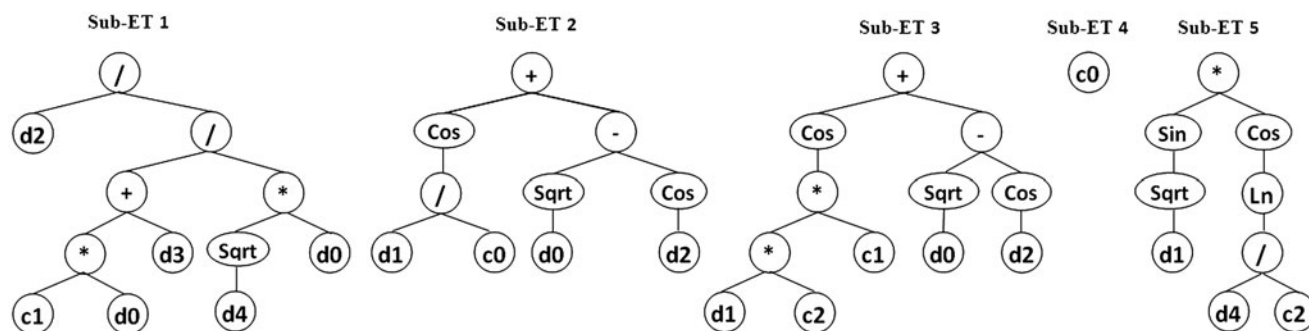
Fig. 4. Expression trees of the GEP model. d0, d1, d2, d3, and d4 indicate C_o, temp., pH, size, and time, respectively.

Table 3
Kinetic parameters for the sorption of BR 46 on WH (pH 10, particle size = 125–250 μm, $m = 1$ g L^{-1}, and $t = 0$–210 min)

	C_o (mg L^{-1})	q_{exp} (mg g^{-1})	Pseudo-second-order kinetic			Logistic			ANN			GEP		
			q_{pred} (mg g^{-1})	R^2	SSE	A (mg g^{-1})	R^2	SSE	q_{pred} (mg g^{-1})	R^2	SSE	q_{pred} (mg g^{-1})	R^2	SSE
293 K	20	16.35	16.94	0.9869	0.5502	19.95	0.9969	0.2690	17.20	0.9925	0.6829	18.60	0.9405	2.5194
	40	25.42	27.33	0.9920	0.7046	29.53	0.9949	0.5603	24.87	0.9961	0.4695	30.44	0.9104	2.4980
	60	30.84	31.82	0.9889	0.9529	36.57	0.9969	0.5036	30.25	0.9942	0.5095	38.24	0.9171	3.4892
	80	35.73	36.92	0.9883	1.1396	44.38	0.9985	0.4059	35.82	0.9989	0.3007	43.98	0.9354	3.8095
	100	40.34	41.87	0.9858	1.4249	51.23	0.997	0.6505	41.19	0.9972	0.5318	48.50	0.9362	3.7873
303 K	20	17.51	17.92	0.9843	1.6014	21.63	0.9969	0.2805	17.38	0.9924	0.4198	17.51	0.9392	2.0209
	40	27.64	29.89	0.9852	1.8369	35.77	0.9938	0.6722	27.01	0.9963	0.4291	27.64	0.9418	2.2050
	60	34.54	35.49	0.9794	2.0595	45.17	0.9951	0.7016	34.81	0.9957	0.5191	34.54	0.9344	2.7529
	80	39.34	39.83	0.9786	2.2245	53.19	0.9971	0.6112	39.88	0.9982	0.3391	39.34	0.9421	3.0983
	100	44.15	44.95	0.9816	2.2958	57.44	0.9972	0.6793	44.76	0.9977	0.4607	44.15	0.9355	3.0516
313 K	20	15.21	18.86	0.9756	0.8273	26.35	0.9974	0.2709	18.61	0.9971	0.2774	18.79	0.9568	1.7924
	40	27.35	32.80	0.9844	1.1705	38.83	0.9938	0.7369	31.14	0.9991	0.2303	30.93	0.9275	2.0790
	60	34.10	38.31	0.9867	1.2405	45.51	0.9983	0.4505	37.80	0.9962	0.6039	37.68	0.9172	3.1774
	80	39.27	42.78	0.9775	1.7935	58.15	0.9981	0.5168	43.75	0.9968	0.4559	42.85	0.9391	3.3285
	100	44.76	48.31	0.9765	2.0721	66.45	0.9978	0.6389	47.56	0.9988	0.5848	48.34	0.9391	3.7237
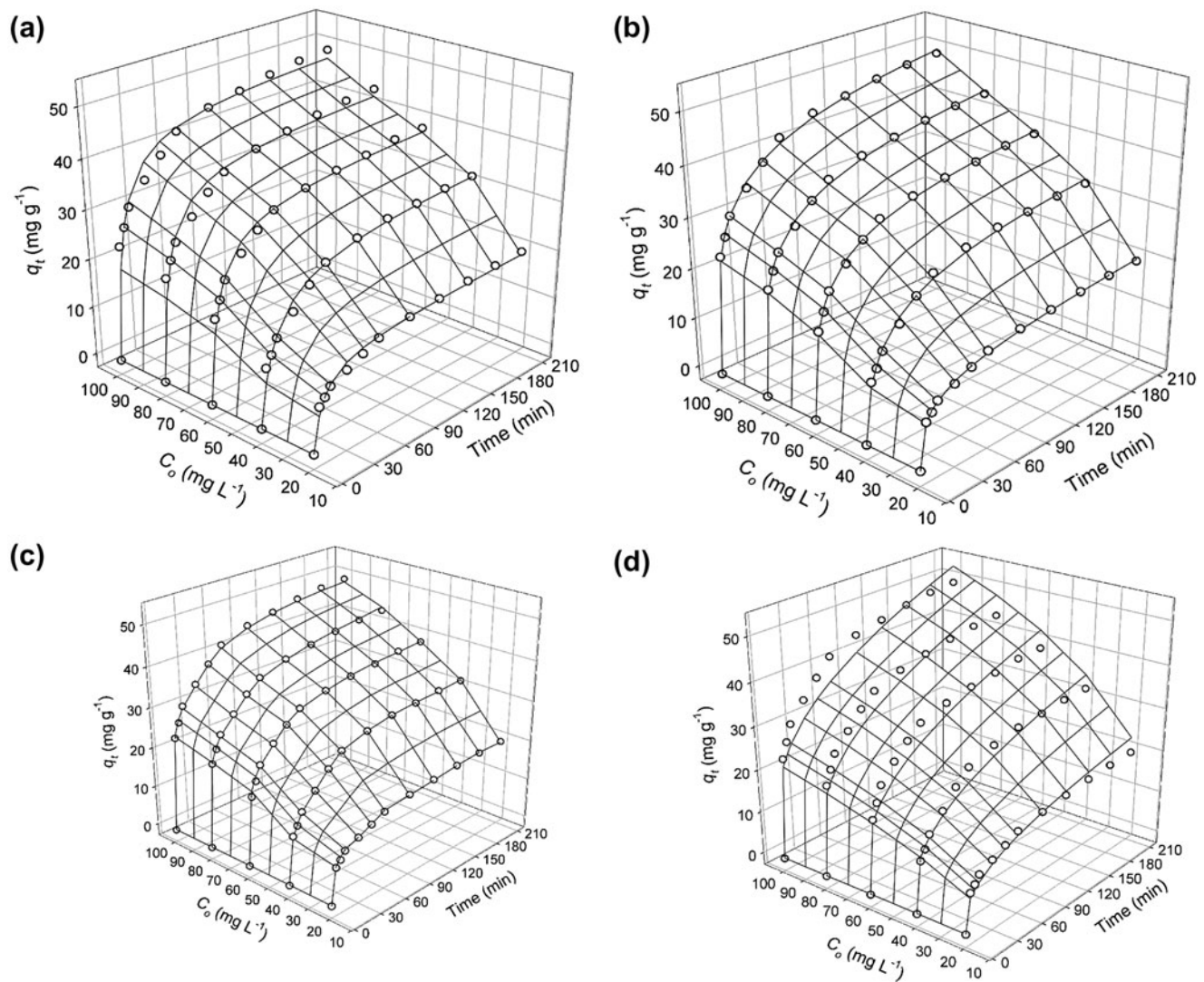
Fig. 5. Comparison of the experimental data with predicted data from (a) pseudo-second-order kinetic, (b) logistic, (c) ANN, and (d) GEP models (pH 10, particle size = 125 µm, C_o = 20–100 mg L^{-1}, t = 0–210 min, and temperature = 313 K).

Table 4
The maximum adsorption capacities of various adsorbents for BR 46

Adsorbent	pH	C_o (mg g^{-1})	q_m (mg g^{-1})	Refs.
Wild olive cores	9	100	88.18	[29]
Canola hull	8	100	23.04	[30]
Princess tree leaf	8	100	46.13	[31]
Moroccan clay	12	28	49.31	[33]
Boron waste	9	300	74.73	[34]
WH	10	100	66.45	This study

and $R^2 = 0.996$ for the removal of reactive orange 12 by copper sulfide nanoparticles-activated carbon [40].

Results indicated that ANN was found to be more suitable model to describe the sorption of BR 46 on *WH*. Moreover, Fig. 5(a)–(d) clearly indicate that ANN had very well agreement with experimental q_t values at all dye concentrations than those of other used models. The highest compatibility of ANN to describe the experimental data was also observed in previous studies [17,20,23,24].

3.4.4. Importance of operating factors from ANN

In order to evaluate the relative importance of various operating variables on output variables, neural net weight matrix [18] was used. Contact time with a relative importance of 48% appeared to be the most influential parameter in the sorption process of BR 46 on *WH*, followed by initial dye concentration (40%), particle size (5%), pH regime (4%), and temperature (3%). The most important input variables on the sorption process varied in the literature, such as contact time for biotreatment of Malachite Green by macroalga [22,23], initial dye concentration (41.43%) for sorption of Acid Black 172 on nonviable *Penicillium* YW 01 [24], contact time (31.16%) for biotreatment of Malachite Green by *Vaucheria* species [41], pH (23%) for the removal of methylene blue on the lignite [39], and pH (43%) for the removal of Lanaset Red G on *WH* [17].

3.4.5. Development of GEP equation for further prediction areas

Sorption system having specific operating conditions can be modeled by the development of an appropriate approach. Although ANN was the best model, all the operation conditions were not included in a single equation. For this purpose, GEP model was developed and applied to include effects of pH, adsorbent particle size, temperature, initial dye concentration, and contact time in a single equation (Eq. (7)). Fitting result of this model is given in Fig. 5(d), which revealed that predicted ($q_{predict}$) values were well agreed with the experimental q_{exp} values. The highest deviation was found from GEP at the higher initial dye concentrations. This case was also observed from the values of SSE. Results of GEP are given in Table 3. Relatively high determination coefficients ($R^2 = 0.957$) show that this model given in Eq. (7) can be used to describe the effects of pH, adsorbent particle size, initial dye concentration, contact time, and temperature on the sorption of BR 46 by *WH*.

The compatibility of GEP modeling to describe the experimental data was observed in previous studies in different works [42,43]. In these works, good coefficient of determinations were reported, in which the $R^2 = 0.90$ for predicting the crushing strength of cold-bonded artificial aggregates [42], 0.90 for predicting effect of nanoparticles on compressive strength of ash-based geopolymers [43]. In sorption study, it was also reported as $R^2 = 0.98$ for the prediction of an azo-metal complex dye onto lentil straw [37]. Additionally, genetic algorithms were used together with ANN in some sorption works, in which $R^2 = 0.97$ for the description of metal ions sorption on chitosan foamed structure-equilibrium [44], $R^2 = 0.99$ for the removal of reactive orange 12 by copper sulfide nanoparticles-activated carbon [41].

3.4.6. Thermodynamic parameters

In order to evaluate the sorption process whether it is spontaneous or not and exothermic or endothermic, thermodynamic parameters [standard free energy changes ($\Delta G°$, kJ mol^{-1}), enthalpy changes ($\Delta H°$, kJ mol^{-1}), and entropy changes ($\Delta S°$, J mol^{-1} K^{-1})] were determined by following equations:

$$\Delta G° = -RT \ln (K_L) \tag{13}$$

$$\Delta G° = \Delta H° - T\Delta S° \tag{14}$$

where R is the universal gas constant (8.314 J mol^{-1} K), T is temperature (K), and K_L is Langmuir constant (L mol^{-1}). Values of $\Delta H°$ and $\Delta S°$ can be determined from the slope and intercept of a plot of ln K_L vs $1/T$ (not shown). Results are given in Table 5. Positive value of $\Delta H°$ indicated that the sorption process was endothermic. Variation in free energy between -20 and 0 kJ mol^{-1} indicated physical sorption, whereas the energy ranging from -80 to -400 kJ mol^{-1} shows chemical sorption. Values of $\Delta G°$ varied from -25.875 to -29.465 kJ mol^{-1}, indicated that the sorption process

Table 5
Thermodynamic parameters for sorption process of dye on adsorbent at different temperatures ($C_o = 20$–200 mg L^{-1}, pH 10, particle size = 125–250 µm, $m = 1$ g L^{-1}, and $t = 210$ min)

T (K)	$\Delta G°$ (kJ mol^{-1})	$\Delta H°$ (kJ mol^{-1})	$\Delta S°$ (kJ mol^{-1} K^{-1})
293	-25.875	26.805	0.179
303	-27.426		
313	-29.465		

for both the adsorbents were mainly physical. Besides, negative value of $\Delta G°$ indicated in this process is being feasible and represents spontaneous nature of sorption.

4. Conclusions

Results revealed that *WH* had a great potential to remove BR 46 from aqueous solution at different environmental conditions. ANN was found to be the best model which showed that contact time was the most efficient parameter, followed by initial dye concentration for the sorption process. GEP model successfully described the sorption process as a function of pH, adsorbent particle size, initial dye concentration, contact time, and temperature in a single equation. As a result, ANN and GEP models can be used in design and scale up for removing of BR 46 on the *WH*.

Acknowledgments

References

[1] V.K. Gupta, R. Kumar, A. Nayak, T.A. Saleh, M.A. Barakat, Adsorptive removal of dyes from aqueous solution onto carbon nanotubes: A review, Adv. Colloid Interface. Sci. 193–194 (2013) 24–34.

[2] R.G. Saratale, G.D. Saratale, J.S. Chang, S.P. Govindwar, Bacterial decolorization and degradation of azo dyes: A review, J. Taiwan Inst. Chem. Eng. 42 (2011) 138–157.

[3] M. Solís, A. Solís, H.I. Pérez, N. Manjarrez, M. Flores, Microbial decolouration of azo dyes: A review, Process Biochem. 47 (2012) 1723–1748.

[4] T. Santhi, S. Manonmani, Malachite green removal from aqueous solution by the peel of Cucumis sativa fruit, Clean 39 (2011) 162–170.

[5] O.S. Bello, K.A. Adegoke, A.A. Olaniyan, H. Abdulazeez, Dye adsorption using biomass wastes and natural adsorbents: Overview and future prospects, Desalin. Water Treat. 53 (2015) 1292–1315.

[6] V.K. Gupta, R. Jain, M. Shrivastava, Adsorptive removal of Cyanosine from waste water using coconut husks, J. Colloid Interface. Sci. 347 (2010) 309–314.

[7] A. Çelekli, B. Tanrıverdi, H. Bozkurt, Lentil straw: A novel adsorbent for removing of hazardous dye— sorption behavior studies, Clean 40 (2012) 515–522.

[8] A. Çelekli, H. Bozkurt, Predictive modeling of an azo metal complex dye sorption by pumpkin husk, Environ. Sci. Pollut. Res. 20 (2013) 7355–7366.

[9] Z. Zhang, I.M. O'Hara, G.A. Kent, W.O.S. Doherty, Comparative study on adsorption of two cationic dyes by milled sugarcane bagasse, Ind. Crops Prod. 42 (2013) 41–49.

[10] S. Nausheen, H.N. Bhatti, Z. Furrukh, S. Sadaf, S. Noreen, Adsorptive removal of Drimarine Red HF-3D dye from aqueous solution using low-cost agricultural waste: Batch and column study, Chem. Ecol. 30 (2014) 376–392.

[11] S. Noreen, H.N. Bhatti, Fitting of equilibrium and kinetic data for the removal of Novacron Orange P-2R by sugarcane bagasse, J. Ind. Eng. Chem. 20 (2014) 1684–1692.

[12] S. Sadaf, H.N. Bhatti, Evaluation of peanut husk as a novel, low cost biosorbent for the removal of Indosol Orange RSN dye from aqueous solutions: Batch and fixed bed studies, Clean Technol. Environ. Policy. 16 (2014) 527–544.

[13] X.S. Wang, Z.Z. Li, S.R. Tao, Removal of chromium (VI) from aqueous solution using walnut hull, J. Environ. Manage. 90 (2009) 721–729.

[14] T. Altun, E. Pehlivan, Removal of Cr(VI) from aqueous solutions by modified walnut shells, Food Chem. 132 (2012) 693–700.

[15] D. Ding, Y. Zhao, S. Yang, W. Shi, Z. Zhang, Z. Lei, Y. Yang, Adsorption of cesium from aqueous solution using agricultural residue – walnut shell: Equilibrium, kinetic and thermodynamic modeling studies, Water Res. 47 (2013) 2563–2571.

[16] J. Yang, K. Qiu, Preparation of activated carbons from walnut shells via vacuum chemical activation and their application for methylene blue removal, Chem. Eng. J. 165 (2010) 209–217.

[17] A. Çelekli, S.S. Birecikligil, F. Geyik, H. Bozkurt, Prediction of removal efficiency of Lanaset Red G on walnut husk using artificial neural network model, Bioresour. Technol. 103 (2012) 64–70.

[18] A.R. Khataee, M.B. Kasiri, Artificial neural networks modeling of contaminated water treatment processes by homogeneous and heterogeneous nanocatalysis, J. Mol. Catal. A: Chem. 331 (2010) 86–100.

[19] L. Cavas, Z. Karabay, H. Alyuruk, H. Doğan, G.K. Demir, Thomas and artificial neural network models for the fixed-bed adsorption of methylene blue by a beach waste *Posidonia oceanica* (L.) dead leaves, Chem. Eng. J. 171 (2011) 557–562.

[20] A. Çelekli, F. Geyik, Artificial neural networks (ANN) approach for modeling of removal of Lanaset Red G on *Chara contraria*, Bioresour. Technol. 102 (2011) 5634–5638.

[21] B. Balci, O. Keskinkan, M. Avci, Use of BDST and an ANN model for prediction of dye adsorption efficiency of *Eucalyptus camaldulensis* barks in fixed-bed system, Expert Syst. Appl. 38 (2011) 949–956.

[22] A.R. Khataee, G. Dehghan, A. Ebadi, M. Zarei, M. Pourhassan, Biological treatment of a dye solution by macroalgae *Chara* sp.: Effect of operational parameters, intermediates identification and artificial neural network modeling, Bioresour. Technol. 101 (2010) 2252–2258.

[23] A.R. Khataee, G. Dehghan, M. Zarei, E. Ebadi, M. Pourhassan, Neural network modeling of biotreatment of triphenylmethane dye solution by a green macroalgae, Chem. Eng. Res. Des. 89 (2011) 172–178.

[24] Y. Yang, G. Wang, B. Wang, Z. Li, X. Jia, Q. Zhou, Y. Zhao, Biosorption of acid black 172 and Congo red

from aqueous solution by nonviable *Penicillium* YW 01: Kinetic study, equilibrium isotherm and artificial neural network modeling, Bioresour. Technol. 102 (2011) 828–834.

[25] C. Ferreira, Gene expression programming: A new adaptive algorithm for solving problems, Complex Syst. 13 (2001) 87–129.

[26] A. Çelekli, H. Bozkurt, F. Geyik, Use of artificial neural networks and genetic algorithms for prediction of sorption of an azo-metal complex dye onto lentil straw, Bioresour. Technol. 129 (2013) 396–401.

[27] Y.S. Ho, G. McKay, Pseudo second-order model for sorption processes, Process Biochem. 34 (1999) 451–465.

[28] A. Çelekli, M. Yavuzatmaca, H. Bozkurt, An eco-friendly process: Predictive modelling of copper adsorption from aqueous solution on *Spirulina platensis*, J. Hazard. Mater. 173 (2010) 123–129.

[29] F. Kaouah, S. Boumaza, T. Berrama, M. Trari, Z. Bendjama, Preparation and characterization of activated carbon from wild olive cores (oleaster) by H_3PO_4 for the removal of Basic Red 46, J. Clean. Prod. 54 (2013) 296–306.

[30] N.M. Mahmoodi, M. Arami, H. Bahrami, S. Khorramfar, Novel biosorbent (Canola hull): Surface characterization and dye removal ability at different cationic dye concentrations, Desalination 264 (2010) 134–142.

[31] F. Deniz, S.D. Saygideger, Removal of a hazardous azo dye (Basic Red 46) from aqueous solution by princess tree leaf, Desalination 268 (2011) 6–11.

[32] L. Wang, J. Zhang, R. Zhao, C. Li, Y. Li, C. Zhang, Adsorption of basic dyes on activated carbon prepared from *Polygonum orientale* Linn: Equilibrium, kinetic and thermodynamic studies, Desalination 254 (2010) 68–74.

[33] A.B. Karim, B. Mounir, M. Hachkar, M. Bakasse, A. Yaacoubi, Removal of Basic Red 46 dye from aqueous solution by adsorption onto Moroccan clay, J. Hazard. Mater. 168 (2009) 304–309.

[34] A. Olgun, N. Atar, Equilibrium and kinetic adsorption study of Basic Yellow 28 and Basic Red 46 by a boron industry waste, J. Hazard. Mater. 161 (2009) 148–156.

[35] A.R. Khataee, A. Movafeghi, S.Torbati, S.Y.S. Lisar, M. Zarei, Phytoremediation potential of duck weed (*Lemna minor* L.) in degradation of C.I. Acid Blue 92: Artificial neural network modeling, Ecotoxicol. Environ. Saf. 80 (2012) 291–298.

[36] S. Elemen, E.P. Akçakoca Kumbasar, S. Yapar, Modeling the adsorption of textile dye on organoclay using an artificial neural network, Dyes Pigm. 95 (2012) 102–111.

[37] A. Çelekli, H. Bozkurt, F. Geyik, Use of artificial neural networks and genetic algorithms for prediction of sorption of an azo-metal complex dye onto lentil straw, Bioresour. Technol. 129 (2013) 396–401.

[38] H. Karimi, M. Ghaedi, Application of artificial neural network and genetic algorithm to modeling and optimization of removal of methylene blue using activated carbon, J. Ind. Eng. Chem. 20 (2014) 2471–2476.

[39] A. Hassani, F. Vafaei, S. Karaca, A.R. Khataee, Adsorption of a cationic dye from aqueous solution using Turkish lignite: Kinetic, isotherm, thermodynamic studies and neural network modeling, J. Ind. Eng. Chem. 20 (2014) 2615–2624.

[40] M. Ghaedi, A.M. Ghaedi, F. Abdi, M. Roosta, R. Sahraei, A. Daneshfar, Principal component analysis-artificial neural network and genetic algorithm optimization for removal of reactive orange 12 by copper sulfide nanoparticles-activated carbon, J. Ind. Eng. Chem. 20 (2014) 787–795.

[41] A.R. Khataee, M. Zarei, G. Dehghan, E. Ebadi, M. Pourhassan, Biotreatment of a triphenylmethane dye solution using a Xanthophyta alga: Modeling of key factors by neural network, J. Taiwan Inst. Chem. Eng. 42 (2011) 380–386.

[42] F. Geyik, M. Gesoğlu, E. Güneyisi, K. Mermerdaş, H.Ö. Öz, Predicting the crushing strength of cold-bonded artificial aggregates by genetic algorithms, in: R.L. Mersky (Ed.), Proceedings of the 27th International Conference on Solid Waste Technology and Management, Philadelphia, USA, 2012, pp. 276–283.

[43] A. Nazari, S. Riahi, Predicting the effects of nanoparticles on compressive strength of ash-based geopolymers by gene expression programming, Neural Comput. Appl. 23 (2013) 1677–1685.

[44] E. Tomczak, Application of ANN and EA for description of metal ions sorption on chitosan foamed structure—equilibrium and dynamics of packed column, Comput. Chem. Eng. 35 (2011) 226–235.